

Probabilistic Assessment of Slope Stability That Considers the Spatial Variability of Soil Properties

Sung Eun Cho, Ph.D.¹

Abstract: In this paper, a numerical procedure for probabilistic slope stability analysis is presented. This procedure extends the traditional limit equilibrium method of slices to a probabilistic approach that accounts for the uncertainties and spatial variation of the soil strength parameters. In this study, two-dimensional random fields were generated based on a Karhunen-Loève expansion in a fashion consistent with a specified marginal distribution function and an autocorrelation function. A Monte Carlo simulation was then used to determine the statistical response based on the generated random fields. This approach makes no assumption about the critical failure surface. Rather, the critical failure surface corresponding to the input random fields of soil properties is searched during the process of analysis. A series of analyses was performed to verify the application potential of the proposed method and to study the effects of uncertainty due to the spatial heterogeneity on the stability of slope. The results show that the proposed method can efficiently consider the various failure mechanisms caused by the spatial variability of soil property in the probabilistic slope stability assessment.

DOI: 10.1061/(ASCE)GT.1943-5606.0000309

CE Database subject headings: Slope stability; Monte Carlo method; Probability; Failures; Limit equilibrium; Soil properties.

Author keywords: Slope stability; Monte Carlo method; Probability; Failures; Limit equilibrium.

Introduction

The slope stability problem can be considered as a system that has many potential failure surfaces. However, the determination of the exact system reliability of the slope stability problem is not possible. Therefore, the probability of failure for the most critical slip surface is commonly used as the estimate for the system failure probability. This approach assumes that the probability of failure along different slip surfaces is highly correlated (Chowdhury and Xu 1995). For the case of highly correlated modes, the contribution to the system failure probability from failure surfaces other than that associated with the maximum failure probability may be small, even though they are infinitely many (Cornell 1967).

The common approaches to a probabilistic analysis are to locate the critical deterministic surface and then calculate the probability of failure that corresponds to this surface. However, the surface of the minimum factor of safety may not be the surface of the maximum probability of failure (Hassan and Wolff 1999). As an alternative, the critical probabilistic surface that is associated with the highest probability of failure or the lowest reliability could be considered (Li and Lumb 1987; Chowdhury and Xu 1995; Bhattacharya et al. 2003; Li and Cheung 2001).

Soil properties vary spatially, even within homogeneous layers, as a result of the depositional and postdepositional processes (Lacasse and Nadim 1996). Therefore, recent studies have con-

sidered the spatial fluctuations of a parameter by using random field theory (El-Ramly et al. 2002; Griffiths and Fenton 2004; Cho 2007).

Griffiths and Fenton (2004) studied slope stabilities by using the random finite-element method (RFEM), which combines the strength reduction method with random fields that are generated by using the local average subdivision method. In the context of the RFEM, a random field of shear strength is generated and mapped onto the finite-element mesh before carrying out the strength reduction analysis. The critical failure mechanism is then determined in the process of analysis since the algorithm seeks out the most critical path through the generated heterogeneous soil mass without assuming the shape and location of the failure surface a priori (Griffiths et al. 2009). Although the RFEM has an advantage in assuming no failure mechanism, the method suffers from excessive computational efforts since the strength reduction method calculates the factor of safety by progressively reducing or increasing the shear strength of the material in order to bring the slope to a state of limiting equilibrium.

The majority of probabilistic slope stability analyses usually employ the traditional limit equilibrium method (LEM). At the early stages of the studies, each soil parameter was modeled by only a single random variable (Low et al. 1998; Chowdhury and Xu 1995; Hassan and Wolff 1999). Some investigators have calculated the probability of failure by using the LEM to consider the spatial variability of the soil properties (Li and Lumb 1987; El-Ramly et al. 2002; Cho 2007). However, when the traditional LEM is combined with the random field theory, the influence of the random field is only taken into account along the predetermined critical surface since the location where the shear strength is calculated continuously changes in the process of searching the critical failure surface. The LEM is simple and is therefore suitable for the Monte Carlo simulation. However, the method requires a random field simulation method that is independent of the division of slices in the sliding mass in order to be able to

¹Senior Researcher, K-Water Institute, Korea Water Resources Corporation, 462-1, Jeonmin-Dong, Yuseong-Gu, Daejeon 305-730, South Korea. E-mail: drsecho@hanmail.net

Note. This manuscript was submitted on July 29, 2009; approved on December 20, 2009; published online on December 28, 2009. Discussion period open until December 1, 2010; separate discussions must be submitted for individual papers. This paper is part of the *Journal of Geotechnical and Geoenvironmental Engineering*, Vol. 136, No. 7, July 1, 2010. ©ASCE, ISSN 1090-0241/2010/7-975-984/\$25.00.

calculate the shear strength at any location along the trial slip surface.

In this study, the effect of spatial variability of shear strength on the slope stability was studied by using the random LEM. Random fields of shear strength parameters were generated by the Karhunen-Loève expansion method that is independent of the division of slices. Then, statistical responses were obtained without assuming a failure mechanism by carrying out a series of limit equilibrium analysis based on a search algorithm that can find the critical failure surface for the generated random fields. The application of the procedure is illustrated below through example problems.

Deterministic Slope Stability Analysis

LEM

Slope stability problems are commonly analyzed by using LEMs of slices. The failing soil mass is divided into a number of vertical slices in order to calculate the factor of safety, which is defined as the ratio of the resisting shear strength to the mobilized shear stress to maintain the static equilibrium. The static equilibrium of the slices and the mass as a whole are used to solve the problem. However, all methods of slices are statically indeterminate and, as a result, require assumptions in order to solve the problem. The approach presented here adopts Bishop's simplified method, which is widely accepted as reasonably accurate and is applicable to the failure surface of a circular shape.

Search for the Critical Failure Surface

LEM requires that the critical failure surface be determined as part of the analysis. The problem of locating the critical circular surface can be formulated as an optimization problem as follows:

$$\min_{\text{surface}} F_s(x_c, y_c, R) \quad (1)$$

where F_s =objective function (the factor of safety); x_c and y_c =coordinates of the center of the circle; and R =radius of the circle.

Although a circular trial slip surface can be described as a function of three shape variables, it could be defined as a series of straight segments. The location of the segment vertices is determined by shape variables and by the location of a hard stratum into which the slip surface cannot penetrate. The treatment for circular slip surface is very simple because there are only three location parameters. Eq. (1) is a type of unconstrained optimization problem that has no equality or inequality conditions. The BFGS method, which is widely acknowledged to be efficient, was applied in this study in order to search for the critical circular slip surface. Kim and Lee (1997) presented a detailed description of this procedure.

Probabilistic Slope Stability Analysis

Limit State Function

The problem of the probabilistic slope stability analysis is formulated by a vector, $\mathbf{X}=[X_1, X_2, X_3, \dots, X_n]$, which represents a set of random variables. From the uncertain variables, a limit state function $g(\mathbf{X})$ is formulated to describe the limit state in the space

of \mathbf{X} . In n -dimensional hyperspace of the basic variables, $g(\mathbf{X})=0$ is the boundary between the region in which the target factor of safety is not exceeded and the region in which it is exceeded.

Cornell (1967) pointed out that a slope is actually a series system with an infinite number of components (or potential modes of failure). Hong and Roh (2008) dealt with the system aspect of the slope in the reliability analysis by defining a limit state of the system as a function of the minimum of the factor of safety for all potential slip surfaces.

If $g_e(\mathbf{X}|s)$ is defined as the limit state function of a single potential slip surface, s , in terms of the factor of safety, $g_e(\mathbf{X}|s)$ can be defined as Eq. (2). Then the limit state function $g(\mathbf{X})$ that considers all potential slip surfaces is defined as Eq. (3). Here

$$g_e(\mathbf{X}|s) = F_s - 1.0 \quad (2)$$

$$g(\mathbf{X}) = \min_{\text{all } s} [g_e(\mathbf{X}|s)] \quad (3)$$

The probability of failure of the slope is then given by the following integral (Baecher and Christian 2003):

$$P_f = P[g(\mathbf{X}) \leq 0] = \int_{g(\mathbf{X}) \leq 0} f_{\mathbf{X}}(\mathbf{X}) d\mathbf{X} \quad (4)$$

where $f_{\mathbf{X}}(\mathbf{X})$ represents the joint probability density function and the integral is carried out over the failure domain.

For slope stability problems, direct evaluation of the n -fold integral is virtually impossible. The difficulty lies in that complete probabilistic information on the soil properties is not available and the domain of integration is a complicated function. Therefore, approximate techniques have been developed to evaluate this integral.

FORM

The first-order reliability evaluation of Eq. (4) is accomplished by transforming the uncertain variables, \mathbf{X} , into uncorrelated standard normal variables, \mathbf{Y} . The primary contribution to the probability integral in Eq. (4) comes from the part of the failure region [$G(\mathbf{Y}) \leq 0$, for which $G(\mathbf{Y})$ is the limit state function in the transformed normal space] closest to the origin. The design point is defined as point \mathbf{Y}^* in the standard normal space located on the limit state function [$G(\mathbf{Y})=0$] with the maximum probability density attached to it. Therefore, the design point, which is the nearest point to the origin in the failure region, is an optimum point at which to approximate the limit state surface. The probability approximated at the design point is

$$P[g(\mathbf{X}) \leq 0] \approx \Phi(-\beta) \quad (5)$$

where β =reliability index defined by the distance from the origin to the design point and Φ =standard normal cumulative density function.

In the first-order reliability method (FORM), a tangent hyperplane is fitted to the limit state surface at the design point. Therefore, the most important and demanding step in the method is finding the design point. The design point is the solution of the following nonlinear constrained optimization problem:

$$\min \|\mathbf{Y}\| \quad \text{subject to } G(\mathbf{Y}) = 0 \quad (6)$$

Monte Carlo Simulation

An alternative means of evaluating the multidimensional integral of Eq. (4) is to use a Monte Carlo simulation. In a Monte Carlo simulation, discrete values of the component random variables are generated in a fashion that is consistent with their probability distribution, and the limit state function is calculated for each generated set. The process is repeated many times to evaluate the probability of failure by determining whether the limit state functions are exceeded. However, the Monte Carlo simulation method is not limited to calculating the probability of failure. Various statistical properties that are evaluated after the process of simulation, such as mean, variance, probability density functions, and cumulative probability distribution functions, can provide a broader perspective and a more comprehensive description of a given slope. Despite the fact that this approach requires excessive computational effort, the mathematical formulation of the Monte Carlo simulation is relatively simple and the method has the capability of handling practically every possible case regardless of its complexity.

Random Field Model

Spatial Variability of Soil

One of the main sources of heterogeneity is inherent spatial soil variability due to different depositional conditions and different loading histories (Elkateb et al. 2003). Statistical parameters, such as the mean and variance, are one-point statistical parameters and cannot capture the features of the spatial structure of the soil (El-Ramly et al. 2002). Spatial variations of soil properties can be effectively described by their correlation structure within the framework of random fields (Vanmarcke 1983).

Autocorrelation distance, defined as the distance to which the autocorrelation function decays to $1/e$ (e is the base of natural logarithms), has been used to describe the spatial extent within which soil properties show a strong correlation. A large autocorrelation distance value implies that the soil property is highly correlated over a large spatial extent, resulting in a smooth variation within the soil profile. On the other hand, a small value indicates that the fluctuation of the soil property is large.

Although an isotropic correlation structure was often assumed in previous studies, correlations in the vertical direction tend to have much shorter distances than those in the horizontal direction due to the geological soil formation process for most natural soil deposits. A ratio of about 1–10 for these autocorrelation distances is considered common (Baecher and Christian 2003).

A Gaussian random field is completely defined by its mean $\mu(x)$, variance $\sigma^2(x)$, and autocorrelation function $\rho(x, x')$. In this study, an exponential autocorrelation function was used and different autocorrelation distances in the vertical and horizontal directions were used as follows:

$$\rho(x, y) = \exp\left(-\frac{|x - x'|}{l_h} - \frac{|y - y'|}{l_v}\right) \quad (7)$$

where l_h and l_v = autocorrelation distances in the horizontal and vertical directions, respectively.

Simulation of Random Fields

Several methods have been developed to carry out this task, such as the spatial average method, the midpoint method, and the

shape function method. These early methods are relatively inefficient in the sense that a large number of random variables are required to achieve a good approximation of the field. More efficient approaches that use series expansion methods such as the Karhunen-Loève expansion and the expansion optimal linear estimation method have been introduced in previous studies (Sudret and Der Kiureghian 2002).

All series expansion methods result in a Gaussian field that is represented exactly as a series that involves random variables and deterministic spatial functions that depend on the correlation structure of the field. The accuracy of the representation depends on the number of terms used in the series expansion and the kind of particular expansion method that is used. In this study, the Karhunen-Loève expansion was adopted to simulate anisotropic random fields of soil properties in two-dimensional space since the method requires the minimum number of terms for a specified level of accuracy compared to other mathematical representations (Ghiocel and Ghanem 2002) and is independent of the division of slices.

Karhunen-Loève Expansion

A random field $H(x, \theta)$ is a collection of random variables associated with a continuous index $x \in \Omega$, where Ω is an open set of R^n describing the system geometry and $\theta \in \Theta$ is the coordinate in the outcome space. The Karhunen-Loève expansion of a random field $H(x, \theta)$ is based on the spectral decomposition of its autocorrelation function $\rho(x, x')$, which is bounded, symmetric, and positive definite. The set of deterministic functions over which any realization of the field $H(x, \theta_0)$ is expanded is defined by the eigenvalue problem as

$$\int_{\Omega} \rho(x, x') \varphi_i(x') d\Omega_{x'} = \lambda_i \varphi_i(x) \quad (8)$$

where φ_i and λ_i denote the eigenfunctions and eigenvalues of the autocorrelation function, respectively.

The series of the deterministic set forms the expansion of $H(x, \theta)$

$$H(x, \theta) = \mu + \sum_{i=1}^{\infty} \sigma \sqrt{\lambda_i} \varphi_i(x) \chi_i(\theta), \quad x \in \Omega \quad (9)$$

where $\chi_i(\theta)$ = set of orthogonal random coefficients (uncorrelated random variables with zero mean and unit variance). The approximate random field is defined by truncating the ordered series given in Eq. (9)

$$\hat{H}(x, \theta) = \mu + \sum_{i=1}^M \sigma \sqrt{\lambda_i} \varphi_i(x) \chi_i(\theta), \quad x \in \Omega \quad (10)$$

The number M to be chosen strongly depends on the desired accuracy and on the autocorrelation function of the random field.

In the case of an exponential autocorrelation function [Eq. (7)] for a one-dimensional case, the eigenvalue problem [Eq. (8)] can be solved analytically. Extension to two-dimensional fields defined for the correlation function on a rectangular domain can be obtained as well. Detailed closed-form solutions can be found in Ghanem and Spanos (1991).

Cross-Correlated Gaussian Random Fields

Typically, more than one random property is involved in geotechnical problems. For example, the cohesion and the friction angle

can be considered as random properties in the problem of slope stability. The present study dealt with cases where all the fields simulated over a region Ω shared an identical autocorrelation function over Ω , and the cross correlation structure between each pair of simulated fields was simply defined by a cross correlation coefficient. This is reasonable since the spatial correlation structure is generally caused by changes in the constitutive nature of the soil over space (Fenton and Griffiths 2003). Therefore, the modal decomposition of the given autocorrelation function is done only once. The cross-correlated fields are then expanded by using the same spectrum of eigenfunctions and eigenvalues, but the sets of random variables used for the expansion of each field are cross correlated.

In this study, each field of cohesion and friction angle was expanded by using a set of independent random variables. These sets are then correlated with respect to the cross correlation matrix between two expanded random fields based on the framework presented by Vořechovský (2008).

Each approximate Gaussian random field \hat{H}_i is then expanded as follows:

$$\hat{H}_i(x, \theta) = \mu_i + \sum_{j=1}^M \sigma_i \sqrt{\lambda_j} \varphi_j(x) \chi_{i,j}(\theta) \quad (\text{for } i = c, \phi) \quad (11)$$

To generate a random field, it is necessary to simulate the correlated random vector $\chi_{i,j}$. In this study, the Latin hypercube sampling technique was used. This technique can be viewed as a stratified sampling scheme designed to ensure that the upper or lower ends of the distributions are well represented.

Transformation to Non-Gaussian Random Fields

Although a Gaussian random field is often used to model uncertainties with spatial variability for reasons of convenience and a lack of available data, the Gaussian model is not applicable in many situations where the random variable is always positive. For convenience, we find an underlying Gaussian random field that can be easily transformed into the target field. If the random variables are considered to be log-normally distributed, then appropriate lognormal random fields can be obtained by exponentiating the approximate Gaussian field from Eq. (11) as follows:

$$\tilde{H}_i(x, \theta) = \exp \left[\mu_i + \sum_{j=1}^M \sigma_i \sqrt{\lambda_j} \varphi_j(x) \chi_{i,j}(\theta) \right] \quad (\text{for } i = c, \phi) \quad (12)$$

Example Analysis

In this section, the application of the presented procedure is illustrated through example problems. For simulations of random field, the solution of eigenvalue problem [Eq. (8)] and the Latin hypercube sampling technique were implemented in Matlab. Then, the simulated random field was used through direct coupling with the slope stability analysis routine written in FORTRAN.

According to the results of a literature review by El-Ramly et al. (2003), the autocorrelation distance is within a range of 10–40 m in the horizontal direction, while in the vertical direction it ranges from 1 to 3 m. As an illustration, an exponential autocorrelation structure with $l_h=20$ m and $l_v=2$ m is used. In this

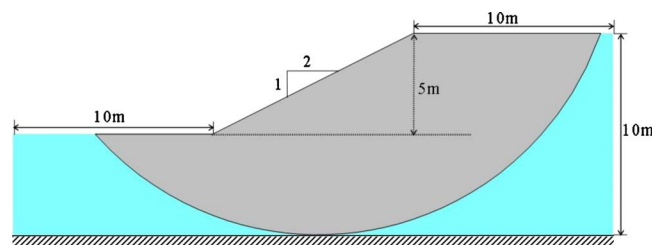


Fig. 1. Example 1: cross section ($F_s=1.356$)

study, the autocorrelation distance l in the Gaussian field was considered in order to maximally exploit the analytical solution of Eq. (8).

All random variables were assumed to be characterized statistically by a lognormal distribution defined by a mean μ_X and a standard deviation σ_X . Once the mean and standard deviation are expressed in terms of the dimensionless coefficient of variation, defined as $\text{COV}_X = \sigma_X / \mu_X$, the mean and standard deviation of the underlying normal distribution of $\ln X$ are then given by

$$\sigma_{\ln X} = \sqrt{\ln\{1 + \text{COV}_X^2\}} \quad (13)$$

$$\mu_{\ln X} = \ln \mu_X - 0.5 \sigma_{\ln X}^2 \quad (14)$$

Example 1: Application to a Saturated Clay Slope under Undrained Conditions ($\phi_u=0$)

In this example, a probabilistic study is performed on an undrained slope with a cross section, as shown in Fig. 1. The undrained shear strength c_u is modeled as a random field. Table 1 summarizes the statistical properties of soil parameters for the slope. The minimum factor of safety that is associated with the critical failure surface based on the mean value of the undrained shear strength is 1.356. The critical deterministic surface is deep and passes through the foundation soil, as shown in Fig. 1. The critical probabilistic surface associated with the maximum probability of failure, as determined by a search of FORM that assumes a perfect spatial correlation, is identical to the critical deterministic surface. The reliability index calculated by FORM is 0.892 and the probability of failure is 0.186.

In the current study, two types of Monte Carlo simulations that considered the spatial variability of soil property were performed. In the first approach, random LEM analysis that determined the critical failure surface based on the search algorithm for each generated random field was carried out in a Monte Carlo simulation. In the second approach, the spatial variability of soil parameters was considered only for the previously located critical surface without considering a search procedure that identifies the critical failure surface in a Monte Carlo simulation.

In order to obtain accurate statistical responses, 100,000 sets of random fields were generated for each case based on the statistical information. A series of analyses was then performed based on the generated random fields.

Table 1. Example 1: Statistical Properties of Soil Parameters

Parameter	μ_X	COV_X
Unit weight γ_{sat} (kN/m ³)	20	—
Undrained shear strength c_u (kPa)	23	0.3

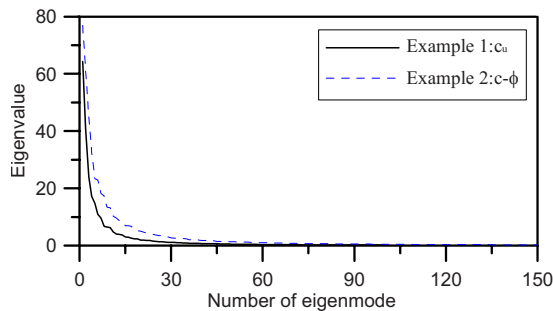


Fig. 2. Eigenvalues of the autocorrelation function ($l_h=20$ m and $l_v=2$ m)

Random fields were generated based on the solutions of the eigenvalue problem. The number of eigenmodes to be retained while simulating a random field depends on the magnitudes of the corresponding eigenvalues. Fig. 2 represents the decaying trends of the eigenvalues obtained by solving the Karhunen-Loève integral eigenvalue problem. In this example, 100 terms of eigenmode were used to represent the random field of undrained shear strength.

As previously explained, a continuous random field can be obtained for an exponential autocorrelation function on a rectangular domain based on the analytical solution of the eigenvalue problem by the Karhunen-Loève expansion method. In other words, the random field simulation is independent of the division of slices. The accuracy of the random field generated by the Karhunen-Loève expansion method depends on the number of terms used in the series expansion, not on the slice width. The slice width in the sliding mass only controls the accuracy of spatial representation of the generated random field.

The influence of the slice division in the sliding mass on the statistical response for the case where $l_h=20$ m, $l_v=2$ m, and $\text{COV}_{c_u}=0.3$ is illustrated in Table 2. With a larger number of

Table 2. Example 1: Influence of Number of Slices on the Statistical Response ($l_h=20$ m, $l_v=2$ m, and $\text{COV}_{c_u}=0.3$)

Number of slices	P_f	μ_{F_s}	σ_{F_s}	COV_{F_s}
45	0.0767	1.2663	0.1993	0.1574
50	0.0763	1.2665	0.1992	0.1573
60	0.0760	1.2669	0.1991	0.1572

slices, the simulated random fields can be better reflected into the limit equilibrium analyses. As indicated in the table, if a sufficient number of slices are used to represent the random field, increasing the number of slices does not significantly alter the responses.

Fig. 3 shows four typical realizations of random field at failure with the searched critical failure surface. In the figures, the lighter regions denote a larger strength parameter value while the darker regions indicate a smaller strength parameter value. These figures show that the failure region developed through the weak strength path in the slope. Various failure surface geometries, caused by the spatial heterogeneity, are not manifested in the deterministic analysis or the probabilistic analysis with a single random variable due to the representation of a homogeneous soil medium.

The results of the simulation are summarized in Fig. 4. Fig. 4(a) shows the convergence of the simulation. As indicated in the figure, the overall probability of failure calculated from the random LEM (0.079) is much greater compared to that obtained for the fixed critical surface (0.032). Fig. 4(b) shows the probability density functions of the factor of safety determined from the two approaches. Fig. 4(c) shows the probability distributions of the factor of safety with the probability of failure obtained from FORM. They indicate that the statistical responses calculated from the Monte Carlo simulations for the two approaches are significantly different. The reason for this is that the random LEM does not assume a particular failure mechanism but searches for the most critical path through the heterogeneous soil mass represented by random field. There are various possible failure mecha-

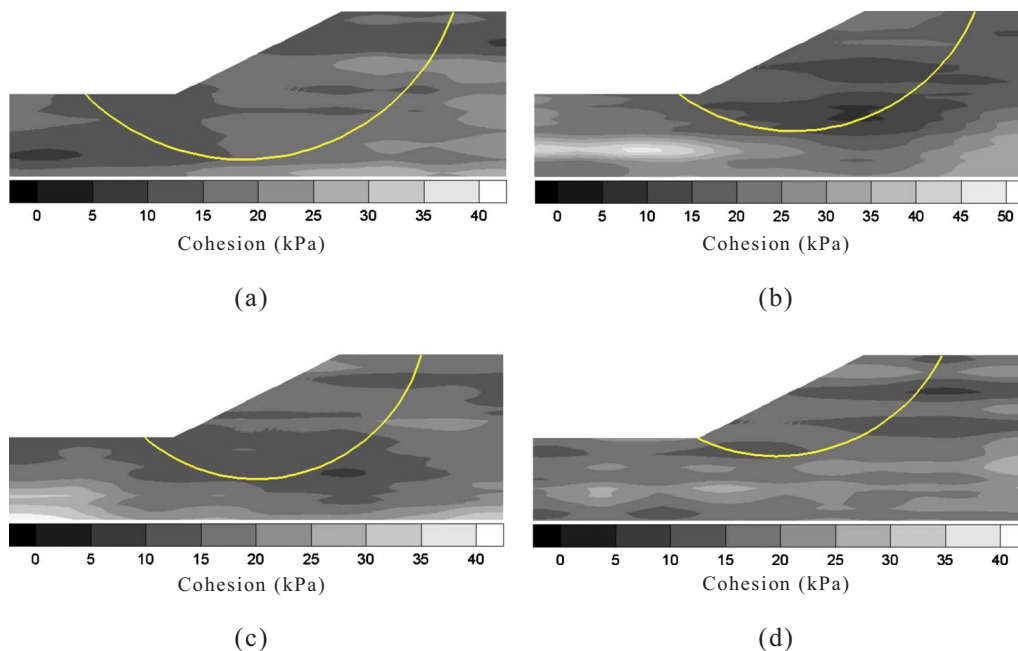


Fig. 3. Example 1: typical realizations of random field and corresponding analysis result ($l_h=20$ m and $l_v=2$ m): (a) $F_s=0.905$; (b) $F_s=0.927$; (c) $F_s=0.834$; and (d) $F_s=0.983$

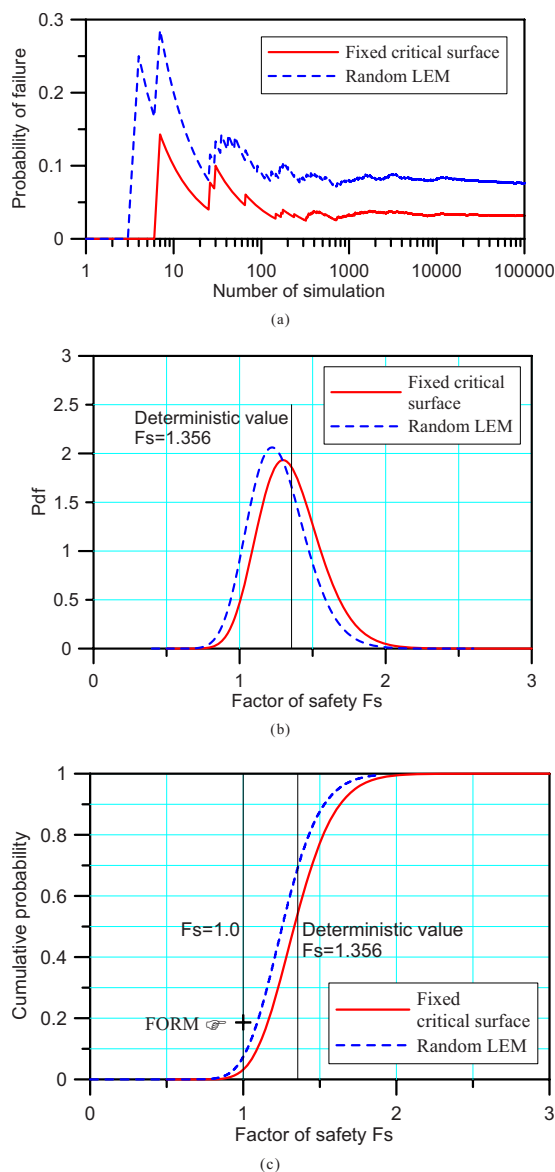


Fig. 4. Example 1: results of the Monte Carlo simulation ($COV_{c_u}=0.3$, $l_h=20$ m, and $l_v=2$ m): (a) convergence of the probability of failure; (b) probability density function; and (c) probability distribution of the factor of safety

nisms for undrained slopes. The failure surface may go through the toe or pass through the deeper foundation soil, as shown in Fig. 3, which leads to a low correlation between the limit state functions of different surfaces. The probability of failure approxi-

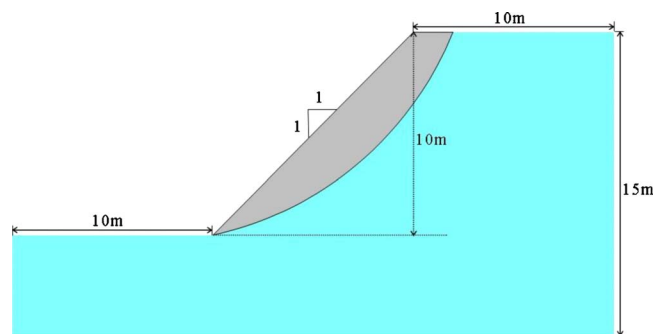


Fig. 5. Example 2: cross section ($F_s=1.204$)

mated by the fixed critical surface is accurate only in cases where the correlation between the safety factors of different surfaces is very high (Cornell 1967).

Table 3 presents summaries of simulation results for cases that have three different sets of autocorrelation distances. The relative difference of the two values of probability of failure was calculated based on the results of the two approaches. As can be noted from the table, the relative difference decreased when the autocorrelation distance increased, which means that the correlation between the limit state functions of different surfaces increased and the failure surfaces by random LEM approached the fixed critical failure surface.

Example 2: Application to a c - ϕ Slope

This example concerns the stability for a c - ϕ slope as presented in Fig. 5. As the strength of the soil is spatially distributed, the friction angle and cohesion are considered as random fields. Statistical moments for these parameters are shown in Table 4.

In order to incorporate the dependence between the strength parameters, the cross correlation coefficient $r(c, \phi)$ is needed. Wolff (1985) reported the correlation between c and ϕ for consolidated-undrained (CU) tests as $r=0.25$ and for consolidated-drained (CD) tests as $r=-0.47$. Yucemen et al. (1973) reported values in a range of $-0.49 \leq r \leq -0.24$, while Lumb (1970) noted values of $-0.7 \leq r \leq -0.37$. A negative correlation implies that low values of cohesion are associated with high values of friction angle and vice versa. In other words, a negative correlation between the cohesion and friction angle means that the uncertainty in the calculated shear strength is smaller than the combined uncertainty in the two-parameter values used to model the shear strength. This observation arises from the fact that the variance of the shear strength is reduced if there is a negative correlation between the cohesion and friction angle (Fenton and

Table 3. Example 1: Summaries of Simulation Results

l_h (m)	l_v (m)	COV_{c_u}	P_f	μ_{F_s}	σ_{F_s}	COV_{F_s}	Relative difference of P_f	
20	2	0.3	0.0316	1.3510	0.2140	0.1584	0.5842	F
			0.0760	1.2669	0.1991	0.1572		S
20	4	0.3	0.0621	1.3528	0.2541	0.1879	0.4308	F
			0.1091	1.2830	0.2430	0.1894		S
40	2	0.3	0.0422	1.3526	0.2301	0.1701	0.5280	F
			0.0894	1.2705	0.2138	0.1683		S

Note: F=Monte Carlo simulation is performed for the fixed critical surface and S=Monte Carlo simulation is performed based on the search algorithm for the critical failure surface.

Table 4. Example 2: Statistical Properties of Soil Parameters

Parameter	μ_X	COV_X	Correlation coefficient
Cohesion c (kPa)	10	0.3	$-0.7 \leq r \leq 0.5$
Friction angle ϕ (degrees)	30	0.2	
Unit weight γ_t (kN/m ³)	20	—	—

Griffiths 2003). In this study, a value of -0.5 is considered as a base set, while the range of $-0.7 \leq r \leq 0.5$ around the base value is considered.

In order to obtain statistical responses, a series of analyses was performed based on the 50,000 sets of random fields generated for each case. In this study 150 terms of eigenmode were used to represent the random fields of cohesion and friction angle (see Fig. 2).

The critical failure surface of the deterministic analysis passes the toe of slope, as shown in Fig. 5, while the factor of safety was estimated to be 1.204. The critical probabilistic surface that was determined by a search of FORM passed through the same surface as the critical deterministic surface. The reliability index was 1.236 and the probability of failure was 0.108.

Fig. 6 shows three typical realizations of random fields at failure with the searched critical failure surface. In the figures, it can be observed that the cohesion and friction angle show a negative correlation while the failure surfaces tend to pass through near the toe.

The results of the Monte Carlo simulation for the case where $r(c, \phi) = -0.5$, $COV_c = 0.3$, $COV_\phi = 0.2$, $l_h = 20$ m, and $l_v = 2$ m are summarized in Fig. 7. Fig. 7(a) shows the overall convergence of the simulations. As indicated in the figure, the overall probability

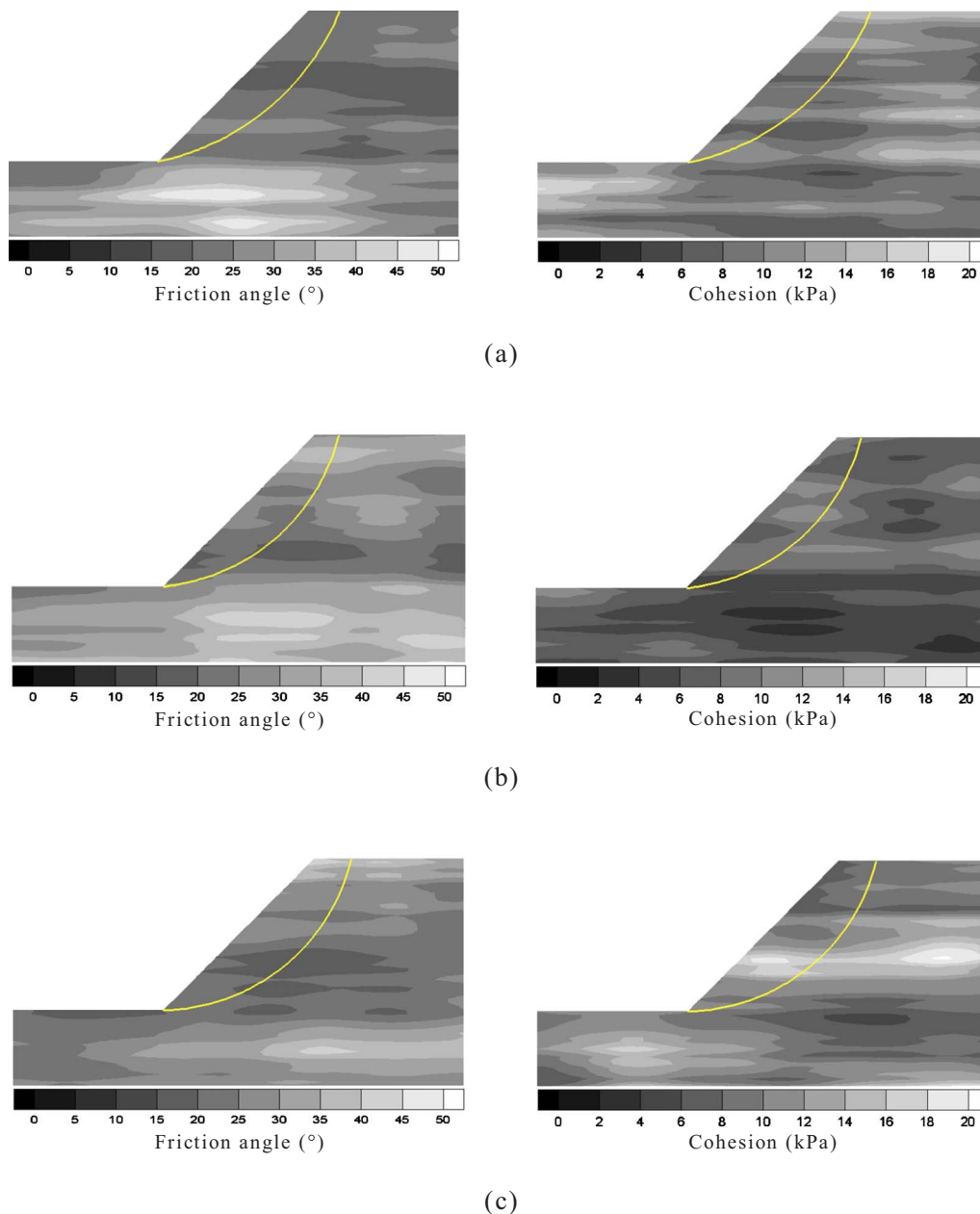


Fig. 6. Example 2: typical realizations of random fields and corresponding analysis result [$r(c, \phi) = -0.5$, $l_h = 20$ m, and $l_v = 2$ m]: (a) $F_s = 0.986$; (b) $F_s = 0.913$; and (c) $F_s = 0.985$

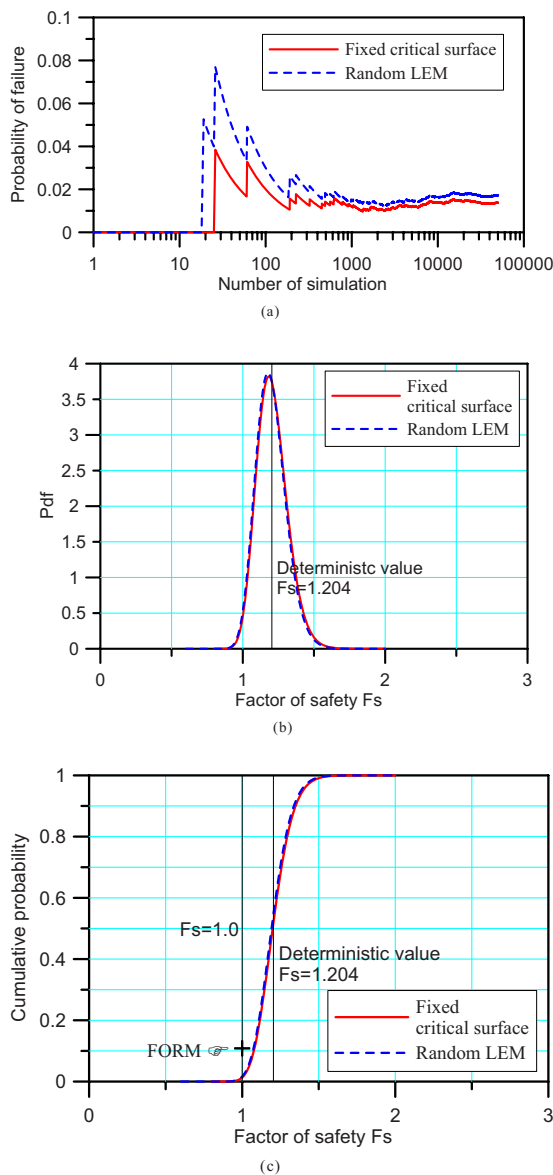


Fig. 7. Example 2: results of the Monte Carlo simulation [$r(c, \phi) = -0.5$, $COV_c = 0.3$, $COV_\phi = 0.2$, $l_h = 20$ m, and $l_v = 2$ m]: (a) convergence of the probability of failure; (b) probability density function; and (c) probability distribution of the factor of safety

of failure calculated from the random LEM (0.0171) is greater compared to that obtained for the fixed critical surface (0.0138), but the difference is not significant. Figs. 7(b and c) show that the probability density functions and the probability distribution of the factor of safety determined from the two approaches are almost identical. The reason for this is that the correlation between the limit state functions of various failure surfaces is very high since, for c - ϕ slopes, the failure mechanism is nearly always shallow and passes through the toe, as shown in Fig. 6.

In this study, the effect of varying the cross correlation between c and ϕ was investigated. Fig. 8(a) shows the effect of cross correlation on the COV of factor of safety. Since the increase of one parameter value decreased the other value, the variation of the total shear strength was reduced, and consequently, the variation of the factor of safety also decreased. An opposite effect for the case of a positive value of the correlation coefficient was also observed. Fig. 8(b) shows the probability

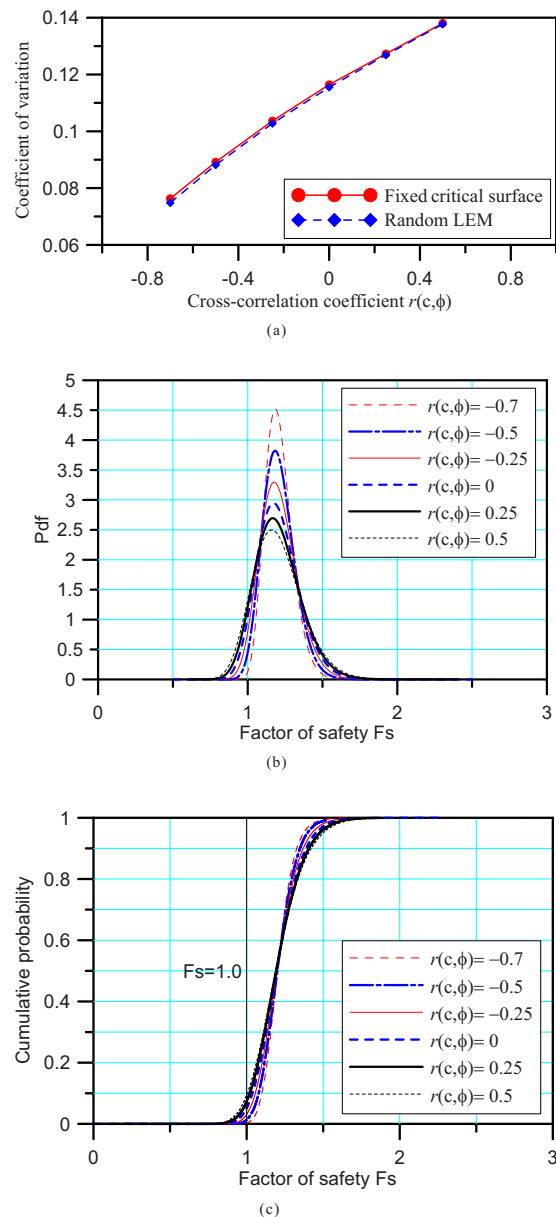


Fig. 8. Example 2: influence of the cross correlation coefficient on the statistical response obtained from simulation ($COV_c = 0.3$, $COV_\phi = 0.2$, $l_h = 20$ m, and $l_v = 2$ m): (a) COV of factor of safety; (b) probability density function (random LEM); and (c) probability distribution of the factor of safety (random LEM)

density functions of the factor of safety that was estimated from the random LEM. The shape of the probability density function becomes narrower and the uncertainty in the factor of safety decreases when the negative value of the cross correlation coefficient increased. The probability distribution estimated from the random LEM also shows the same trend, as shown in Fig. 8(c).

Fig. 9 shows the estimated probability of failure against the cross correlation. The probability of failure decreases when the negative correlation coefficient increases. Therefore, the assumption of independence between the cohesion and friction angle gives conservative results if the actual correlation is negative, but slightly unconservative results are obtained if the actual correlation is positive.

The effects of the autocorrelation distance on simulation results are summarized in Table 5. As indicated in the table, when

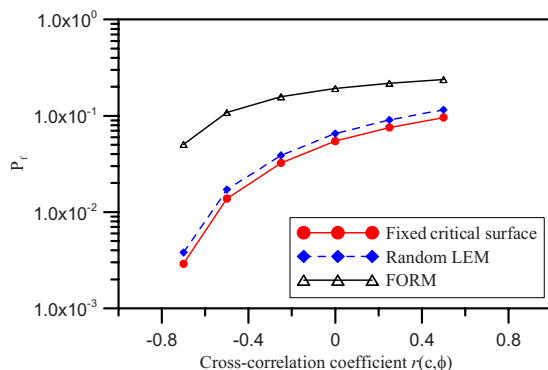


Fig. 9. Example 2: influence of the cross correlation on the probability of failure (FORM assumes a single random variable)

the autocorrelation distance increased, the relative difference between the overall probability of failure and the probability of failure associated with the fixed critical surface decreases. This means that the failure mechanisms by random LEM approach the fixed critical surface. The results also show that the vertical autocorrelation distance has greater influence on the statistical response.

Discussions

Finding the critical slip surface that gives the lowest factor of safety is one of the key issues in any limit equilibrium stability analysis. Stratigraphic conditions have a major influence on potential slip surfaces. A simple circular failure surface method is sufficient for a slope in a homogenous soil layer, while for a heterogeneous multisoil layer slope, a noncircular failure surface method should be considered as circular methods can overpredict the factor of safety (Zolfaghari et al. 2005).

In this section, stability analysis based on the strength reduction method is conducted by FLAC to show that the use of circular surfaces is a reasonable approximation for the studied problem (Example 1). Strength reduction method can provide an alternative to the LEM in providing an assessment of the stability of slopes. The main advantage of the strength reduction method is that it requires no assumption on the shape or location of the failure surface. The critical failure surface is determined automatically from the shear strain arising from the reduction of shear strength. FLAC uses an explicit time marching method to solve the governing field equations in which every derivative is replaced by an algebraic expression written in terms of the field variables at discrete points in space. To be consistent with the

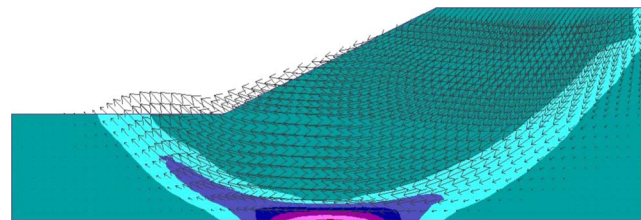


Fig. 10. Example 1: result of the stability analysis by the strength reduction method based on the mean value of the undrained shear strength ($F_s = 1.322$)

conventional LEMs, the calculations are performed within the framework of the elastic-perfectly plastic Mohr-Coulomb model with no hardening or softening. As the strength of the soil is a spatially distributed random variable, soil strength should be modeled as random field considering spatial correlation. A combination of random field and finite difference analysis method was adopted to seek out the more realistic critical path through the soil (Cho and Park 2009).

The minimum factor of safety calculated from a deterministic analysis based on the mean value of the shear strength is 1.322, which is slightly lower than 1.356 from Bishop's simplified method. The plot of the shear strain rate shows that the failure surface is similar to the critical circular surface, as presented in Fig. 10. The arrows in Fig. 10 are velocity vectors, which indicate the pattern of motion at the initiation of failure and show a well-defined circular failure surface. Fig. 11 shows results of the stability analysis by the strength reduction method for the same realizations of random field previously shown in Fig. 3. Fig. 11 shows that the failure surfaces determined by the strength reduction method are quite similar to the critical circular surfaces by Bishop's simplified method although some localized noncircular shape can be observed due to the existence of stratified weak regions. The differences between the factor of safety for the strength reduction method and the factor of safety for LEM are small to be of practical consequence. This suggests that it can be assumed with reasonable accuracy that the critical slip surface is circular in a single-layered slope. However, it is evident that once the anisotropic spatial correlation parameters are incorporated slopes become stratified. Hence, a search for the critical noncircular surface is required. Further refinement of the shape for a circular slip surface can lead to a noncircular slip surface that is attracted to the lower strength horizontal layers, which will result in lower factors of safety and higher probabilities of failure.

In addition, due to the variety of soil types and multilayered soil profiles that exist in real field cases, future studies should also consider multilayer soil effects on probabilistic slope stability

Table 5. Example 2: Summaries of Simulation Results

l_h (m)	l_v (m)	COV		P_f	μ_{F_s}	σ_{F_s}	COV_{F_s}	Relative difference of P_f	
		c	ϕ						
20	2	0.3	0.2	0.0138	1.2072	0.1077	0.0892	0.1930	F
				0.0171	1.1991	0.1057	0.0881		S
20	4	0.3	0.2	0.0323	1.2100	0.1292	0.1068	0.1270	F
				0.0370	1.2015	0.1262	0.1051		S
40	2	0.3	0.2	0.0155	1.2086	0.1108	0.0917	0.1885	F
				0.0191	1.2003	0.1086	0.0905		S

Note: F=Monte Carlo simulation is performed for the fixed critical surface and S=Monte Carlo simulation is performed based on the search algorithm for the critical failure surface.

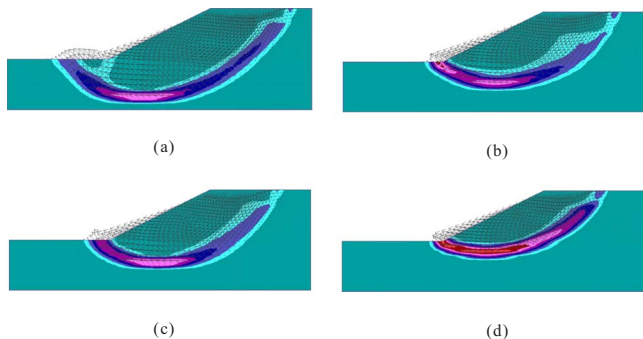


Fig. 11. Example 1: results of the stability analysis by the strength reduction method for the same realizations of random field shown in Fig. 3: (a) $F_s=0.881$; (b) $F_s=0.889$; (c) $F_s=0.811$; and (d) $F_s=0.975$

analysis based on multiscale random fields that varies spatially at a large scale as different zonations due to stratification and also at a smaller scale within each individual zone.

Conclusions

This paper proposed a numerical procedure that considers the slope stability problems with uncertain quantities. The procedure extends the deterministic analysis based on the LEM of slices to a probabilistic approach that accounts for the uncertainties and spatial variation of the soil parameters.

From the example problems of one-layered slope, the following observations can be made:

1. A combination of random field and LEM enables us to efficiently consider the various failure mechanisms caused by the spatial variability of soil property in the probabilistic slope stability assessment by searching for the critical path through the soil.
2. The probability of failure associated with a fixed critical surface was smaller than the overall probability of failure that comprises all potential failure surfaces since the critical failure surface identified by search algorithm always gives a smaller or an equal factor of safety compared to that obtained from the fixed critical surface for each random field.
3. The results also indicate that the overall probability of failure can be significantly higher than the probability of failure associated with a fixed critical slip surface in a saturated clay slope under an undrained condition due to the spatial heterogeneity of shear strength. On the contrary, for c - ϕ slopes the limit state functions of slip surfaces are highly correlated. Hence, the difference between the overall probability of failure and that for the fixed critical surface is not significant.

References

- Baecher, G. B., and Christian, J. T. (2003). *Reliability and statistics in geotechnical engineering*, Wiley, New York.
- Bhattacharya, G., Jana, D., Ojha, S., and Chakraborty, S. (2003). "Direct search for minimum reliability index of earth slopes." *Comput. Geotech.*, 30(6), 455–462.
- Cho, S. E. (2007). "Effects of spatial variability of soil properties on slope stability." *Eng. Geol. (Amsterdam)*, 92(3–4), 97–109.

- Cho, S. E., and Park, H. C. (2009). "Effect of spatial variability of cross-correlated soil properties on bearing capacity of strip footing." *Int. J. Numer. Anal. Meth. Geomech.*, 34(1), 1–26.
- Chowdhury, R. N., and Xu, D. W. (1995). "Geotechnical system reliability of slopes." *Reliab. Eng. Syst. Saf.*, 47(3), 141–151.
- Cornell, C. A. (1967). "Bounds on the reliability of structural systems." *J. Struct. Div.*, 93(1), 171–200.
- El-Ramly, H., Morgenstern, N. R., and Cruden, D. M. (2002). "Probabilistic slope stability analysis for practice." *Can. Geotech. J.*, 39(3), 665–683.
- El-Ramly, H., Morgenstern, N. R., and Cruden, D. M. (2003). "Probabilistic stability analysis of a tailings dyke on presheared clay-shale." *Can. Geotech. J.*, 40(1), 192–208.
- Elkateb, T., Chalaturnyk, R., and Robertson, P. K. (2003). "An overview of soil heterogeneity: Quantification and implications on geotechnical field problems." *Can. Geotech. J.*, 40(1), 1–15.
- Fenton, G. A., and Griffiths, D. V. (2003). "Bearing capacity prediction of spatially random c - ϕ soils." *Can. Geotech. J.*, 40(1), 54–65.
- Ghanem, R. G., and Spanos, P. D. (1991). *Stochastic finite element—A spectral approach*, Springer, New York.
- Ghiocel, D. M., and Ghanem, R. G. (2002). "Stochastic finite-element analysis of seismic soil-structure interaction." *J. Eng. Mech.*, 128(1), 66–77.
- Griffiths, D. V., and Fenton, G. A. (2004). "Probabilistic slope stability analysis by finite elements." *J. Geotech. Geoenviron. Eng.*, 130(5), 507–518.
- Griffiths, D. V., Huang, J., and Fenton, G. A. (2009). "Influence of spatial variability on slope reliability using 2-d random fields." *J. Geotech. Geoenviron. Eng.*, 135(10), 1367–1378.
- Hassan, A. M., and Wolff, T. F. (1999). "Search algorithm for minimum reliability index of earth slopes." *J. Geotech. Geoenviron. Eng.*, 125(4), 301–308.
- Hong, H. P., and Roh, G. (2008). "Reliability evaluation of earth slopes." *J. Geotech. Geoenviron. Eng.*, 134(12), 1700–1705.
- Kim, J. Y., and Lee, S. R. (1997). "An improved search strategy for the critical slip surface using finite element stress fields." *Comput. Geotech.*, 21(4), 295–313.
- Lacasse, S., and Nadim, F. (1996). "Uncertainties in characterizing soil properties." *GSP 58 uncertainty in the geologic environment*, C. D. Shackelford, P. P. Nelson, and M. J. S. Roth, eds., ASCE, Reston, Va., 49–75.
- Li, K. S., and Cheung, R. W. M. (2001). "Search algorithm for minimum reliability index of earth slopes (Discussion)." *J. Geotech. Geoenviron. Eng.*, 127(2), 197–198.
- Li, K. S., and Lumb, P. (1987). "Probabilistic design of slopes." *Can. Geotech. J.*, 24(4), 520–535.
- Low, B. K., Gilbert, R. B., and Wright, S. G. (1998). "Slope reliability analysis using generalized method of slices." *J. Geotech. Geoenviron. Eng.*, 124(4), 350–362.
- Lumb, P. (1970). "Safety factors and the probability distribution of soil strength." *Can. Geotech. J.*, 7(3), 225–242.
- Sudret, B., and Der Kiureghian, A. (2002). "Comparison of finite element reliability methods." *Probab. Eng. Mech.*, 17(4), 337–348.
- Vanmarcke, E. H. (1983). *Random fields: Analysis and synthesis*, MIT Press, Cambridge, Mass.
- Vořechovský, M. (2008). "Simulation of simply cross correlated random fields by series expansion methods." *Struct. Safety*, 30(4), 337–363.
- Wolff, T. H. (1985). "Analysis and design of embankment dam slopes: A probabilistic approach." Ph.D. thesis, Purdue University, Lafayette, Ind.
- Yucemen, M. S., Tang, W. H., and Ang, A. H. S. (1973). *A probabilistic study of safety and design of earth slopes*, Structural Research Series Vol. 402, University of Illinois, Urbana, Ill.
- Zolfaghari, A. R., Heath, A. C., and McCombie, P. F. (2005). "Simple genetic algorithm search for critical non-circular failure surface in slope stability analysis." *Comput. Geotech.*, 32(3), 139–152.